SPATIAL DOWNSCALING OF SMAP SOIL MOISTURE USING THE MODIS AND SRTM OBSERVATIONS

J.D.Mohite[1]*, S.A.Sawant[1], A.Pandit[1], S. Pappula[2]

[1] TCS Research and Innovation, Tata Consultancy Services, Mumbai, India
[2] TCS Research and Innovation, Tata Consultancy Services, Hyderabad, India
(jayant.mohite, suryakant.sawant, ankur.pandit, srinivasu.p)@tcs.com

Commission III, WG 10

KEY WORDS: Soil Moisture, Downscaling, SMAP, Machine Learning, MODIS

ABSTRACT:

The main objective of this study is the spatial downscaling of Soil Moisture Active Passive (SMAP) soil moisture (36 km) using the Moderate Resolution Imaging Spectroradiometer (MODIS) and Shuttle Radar Topography Mission (SRTM) products. The study was conducted over India during the post-monsoon (i.e., *Rabi*) season Daily SMAP soil moisture (SM) data was composited to 3 days to cover the entire study area. MODIS data for the Normalized Difference Vegetation Index (NDVI), Normalized Difference Water Index (NDWI), Albedo, and Land Surface Temperature (LST) were similarly obtained by constructing a three day composite. SMAP soil moisture was used as a dependent variable, whereas, MODIS NDVI, NDWI, Albedo, LST, and SRTM elevation were used as independent variables in a regression analysis for downscaling of SMAP soil moisture. The coefficient of determination (R^2) was used to evaluate the performance of multi-variate linear regression (MLR), support vector regression (SVR), and random forest regression (RFR). Each method was used to test the performance of monthly and seasonal models. RFR outperformed MLR and SVR for monthly and seasonal models. Furthermore, a comparison of monthly and seasonal models revealed that the model created on Jan. data performed best (R^2=0.80), while R^2 of 0.73, 0.61, 0.75, and 0.76 were attained using RFR for seasonal, Dec., Feb., and Mar. models, respectively. In addition, in-situ soil moisture data was used to validate downscaled soil moisture (1 km). Comparison between downscaled soil moisture and in-situ soil moisture showed good agreement with a difference ranging between -9.3 to 7.4 %.

1. INTRODUCTION AND STATE OF THE ART

Soil moisture (SM) is an important variable in the climate system that controls the exchange of water, energy, and carbon fluxes between the land surface and the atmosphere (Ochsner et al., 2013, Robock et al., 2000, Wagner et al., 2007). Hence, SM datasets play a key role in a variety of application domains such as water resource management (Bastiaanssen et al., 2000), hydrology (Robinson et al., 2008), climatology (Anderson et al., 2007), etc. A variety of techniques have been developed in the past for the measurement and monitoring of soil moisture. Laboratory-based methods like the Gravimetric method (Vinnikov and Yeserkepova, 1991) is based on the destruction of soil samples in the laboratory. These methods are time-consuming, labor intensive and cannot be reproduced (Seneviratne et al., 2010). Over the years, various sensors have been developed for SM measurements. Techniques such as Time Domain Reflectometry (TDR) (Ledieu et al., 1986), Capacitance based technique (Dean et al., 1987), neutron probes (Chanasyk and Naeth, 1996) and gamma-ray scanners (Bacchi et al., 1998) have been developed for point-based measurement of SM. However, since the sensors measure the SM at a single point, they cannot be used as an indicator for regional-scale studies (Zhang and Zhou, 2016).

In addition to this, Remote Sensing (RS) based methods provide an alternative way to estimate the spatial soil moisture content using the optical (Multispectral and Hyperspectral), thermal, and microwave datasets of the electromagnetic spectrum. Thermal infrared remote sensing has also been used for SM estimation, mainly due to the proven strong relationship between the thermal properties of soil and SM (Zhang and Zhou, 2016). However, the availability of the thermal infrared data is a challenge due to the high costs associated with the sensor. Multiple attempts have been made to use the optical data for SM estimation. However, the optical satellite observations have limited penetration into the soil, which limits the precision of soil moisture estimation. On the contrary, microwave (active/passive) remote sensing has been used for SM estimation due to its advantages of cloud penetration, all-weather capabilities, etc. (Pandit et al., 2020). Several global microwave SM products have been produced, such as the AMSR-E Land Parameter Retrieval Model (LPRM) (Owe et al., 2008), the ASCAT (Naeimi et al., 2009), the Soil Moisture and Ocean Salinity (SMOS) (Jacquette et al., 2010, Kerr et al., 2001), and the European Space Agency's Climate Change Initiative (ESA CCI) SM products (Liu et al., 2011, Wagner et al., 2012).

While datasets are available at global scales at daily temporal resolution, the spatial resolution of the data is coarse, and limits the usability of the data at a field or local scale. One method for obtaining medium or high resolution SM data is to spatially downscale the SM data. Detailed review of various downscaling techniques was carried out in the past (Peng et al., 2017). The authors grouped the downscaling techniques into three categories, such as satellite based methods, methods based on geoinformation data, and model based methods. Satellite based methods mainly include those based on the fusion of active-passive microwave datasets (Das et al., 2010), fusion of optical/thermal-microwave datasets (Malbéteau et al., 2016). Methods developed based on the geoinformation data

* Corresponding author

consider the fact that SM is related to topographical, soil attribute, and vegetation characteristics (Busch et al., 2012, Coleman and Niemann, 2013). However, these methods are dependent on large in-situ observations. Modeling-based downscaling approaches mainly involve statistical downscaling (Kaheil et al., 2008) or physical process based models (Ines and Droogers, 2002). Due to the limited availability of field level sensor observations needed for physical models, many researchers have developed the machine learning based models (Liu et al., 2017, Sheng et al., 2019).

In this work, SM downscaling has been attempted based on the relationship between vegetation/land characteristics and soil moisture. The main objective of this study is to use the MODIS and SRTM products to downscale SMAP soil moisture (36 km) to 1 km spatial resolution. The study was conducted across India during the post-monsoon (i.e., *Rabi*) season, starting in Nov. and ending in Mar. The study considered *Rabi* seasons data for the year 2017–18, 2018–19, 2019–20, and 2020–21.

2. MATERIALS AND METHODS

2.1 Study Area

This study was carried out on Indian geography. The geographical extent of India lies between 6° 44' and 35° 30' N latitude and 68° 7' and 97° 25' E longitude. In India, agriculture accounts for a significant contribution to the Gross Domestic Product (GDP) (NPI, 2022). The study was carried out during the post-monsoon cropping season. The season is locally called the *Rabi* Season. Crop cultivation is carried out during the three different cropping seasons. The main cropping season is followed by the South-West monsoon (locally called the *Kharif* season). This season starts in Jun.-Jul. and harvesting is completed in Oct.-Nov. month. The second season is the *Rabi* season, during which we have carried out the study. This season starts in Nov.-Dec. and ends in Mar.-Apr. month of subsequent year. The third season, which starts in Mar.-Apr. and ends in May-Jun., is locally called the *Zaid* or summer season. Both the *Rabi* and summer season crops are dependent on supplemental irrigation. Hence, precise and timely monitoring of SM at a local or field scale is critical.

2.2 Datasets Used

This section describes the various datasets used and covers the overall modelling approach followed in this study.

2.2.1 SMAP 36 km Soil Moisture The Level-3 (L3) SM product provides a composite of daily estimates of global land surface conditions retrieved by the Soil Moisture Active Passive (SMAP) passive microwave radiometer (O'Neill et al., 2019). Soil moisture data from SMAP are resampled to a global, cylindrical 36 km Equal-Area Scalable Earth Grid, Version 2.0 (EASE-Grid 2.0). Daily data was downloaded from the NASA's Earthdata portal using the 'smapr' package developed in R (Joseph et al., 2019). Further 3-days compositing was carried out to seamlessly cover the study region.

2.2.2 MODIS Based Indices A 500 m spatial resolution data available from MOD09GA and MYD09GA version 6 surface reflectance product was utilized in this study (Vermote and Wolfe, 2015) . Considering the data from Red, Near-Infrared and Shortwave-Infrared bands of these products, indices such as

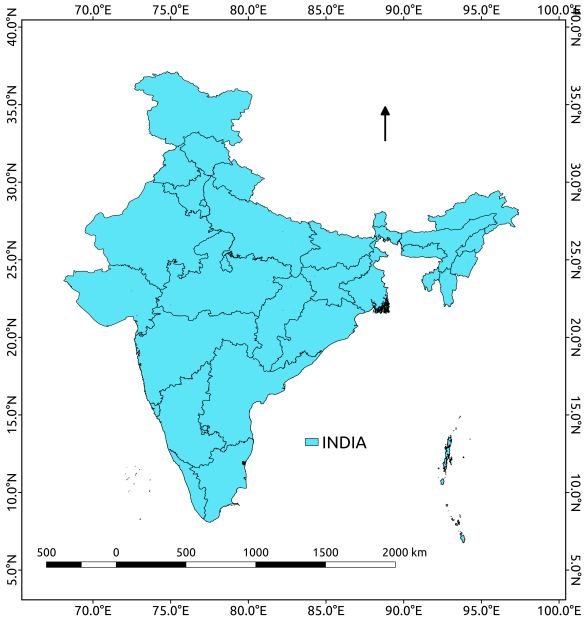

Figure 1. Study area

NDVI, NDWI were estimated. Moreover, Land Surface Temperature (LST) has strong link with the soil moisture hence data available from MOD11A1 and MYD11A1 version 6 products was considered in this study (Schaaf and Wang, 2015). The dataset was available at 1 km spatial resolution. In addition to this, literature reported that, black and white sky albedo data has strong association with SM (Sheng et al., 2019). The data from MCD43A3 version 6 product on black and white sky albedo available at 500 m spatial resolution was used in this study (Wan, 2015). All the MODIS products are available on Google Earth Engine (GEE) (Gorelick et al., 2017). Required data for our study region was accessed from GEE which saved huge amount of time and compute needed for data downloading and processing.

2.2.3 SRTM Digital Elevation Data The Shuttle Radar Topography Mission (SRTM) datasets are the result of a collaborative effort by the National Aeronautics and Space Administration (NASA) and the National Geospatial-Intelligence Agency (NGA)—previously known as the National Imagery and Mapping Agency, or NIMA—as well as the participation of the German and Italian space agencies. The SRTM digital elevation dataset (SRTM90 V4), available at 90 m spatial resolution, was used in this study (Jarvis et al., 2008). The data for the study region was accessed from the GEE platform and analysis was carried out.

2.2.4 In-situ Soil Moisture Data Demo farm which is maintained by Tata Consultancy Services (TCS) Limited, is located in Pune, Maharashtra, India. The location map of the TCS Demo Farm is given in Figure 2. The KDS-042 sensor, developed by Komoline Aerospace Limited, was deployed on the demo farm for in-situ SM measurement and monitoring. Data from node 3 was collected by the sensor at an hourly interval. We have utilised the data collected on selected dates during the period of December 2017 to March 2018 for validation of the models developed in this study.

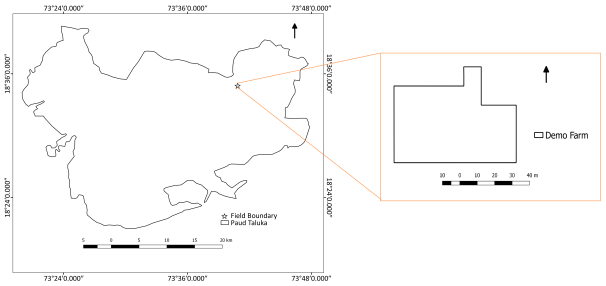

Figure 2. Validation Site: TCS demo farm located in Pune, India

SN	Dataset	Variable	Spatial Resolution (m)	Temporal Resolution (Days)
1	MOD09A1	NDVI	500	1
2	MOD09A1	NDVI	500	1
3	MOD11A	LST	1000	1
4	MCD43A3	Albedo	500	1
5	SRTM	Elevation	90	-
6	SMAP	Soil Moisture	36000	1
6	GFSAD	Agri Mask	30	-

Table 1. Description of datasets used in the study

2.3 Overall Approach

Figure 3 depicts the overall framework used in this work. Machine learning-based regression modelling was carried out where SMAP-based L band data at 36 km spatial resolution was used as the dependant variable. Variables obtained from MODIS data such as NDVI, NDWI, LST, Black and White sky albedo, and SRTM based elevation data were used as independent variables. We have resampled all the independent variables to 36 km to match the spatial resolution of the dependant variable. The entire India geography is considered as study area for downscaling of soil moisture. However, the SMAP data was not available for the entire study area on a daily basis. Hence, 3-day composites were created from dependant and independent variables for the study period, i.e., 1 December to 31 March. Furthermore, the composite stack (CS) was created by stacking all the layers together. We considered the data from the *Rabi* season of 2017–18, 2018–19, 2019–20, and 2020–21. As the study was focused on the agriculture areas, we masked out the non-agriculture areas of the study region. Random 100 points were drawn from the agriculture area of the study region and data for those 100 points was extracted from each of the CS available during the study period. The total number of CS created during the study period was 39 (10 CS each from Dec., Jan., and Mar., and 9 from Feb.). The total sample size for the study seasons was 15600 (4 seasons x 100 points x 39 CS). We evaluated the performance of various well known regression techniques, such as Multiple Linear Regression (MLR), Support Vector Regression (SVR) and Random Forest Regression (RFR), using the data extracted. In the first scenario, we considered all the data together, and random data was selected for model training and testing. However, in the second scenario, models were trained on three seasons (2018–19, 2019–20, and 2020–21) and tested on the remaining season, i.e., 2017–18. For each scenario, models for individual months were developed along with a model based on all months' data. Model performance was measured based on the coefficient of determination (R^2) value obtained for the test dataset. Further, validation using the in-situ sensor data from Demo Farm, Pune, India was also performed.

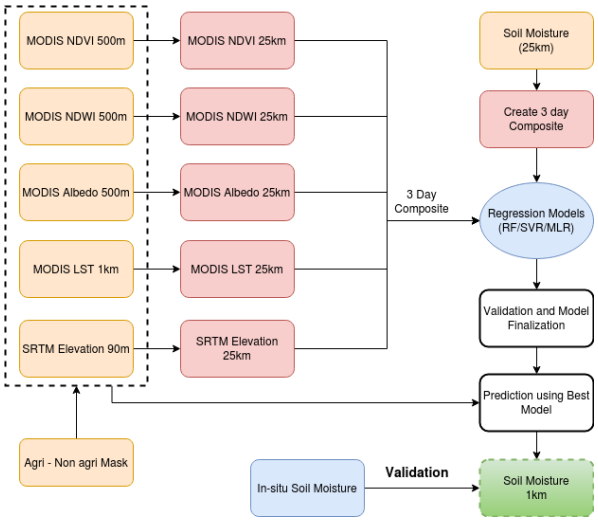

Figure 3. Overall analysis framework

3. RESULTS AND DISCUSSION

This section covers results obtained using various regression models and the validation performed using in-situ SM observations.

3.1 Performance of Various Regression Models

Data for SM, NDVI, NDWI, LST, black sky albedo, white sky albedo, and elevation were extracted from each composite stack. As mentioned in subsection 2.3, 100 samples were extracted from each CS, which totals 15600 samples for the four seasons (2017–18, 2018–19, 2019–20, and 2020–21). In the first scenario, data from all the seasons is considered and divided into two parts, i.e., training and testing. 80 % of the data was used for model training, and the remaining 20 % data was used for model testing. However, in the second scenario, we have used data from three seasons, viz., 2018–19, 2019–20, and 2020–21. Model training was carried out on 80 % of the data, and 20 % data was used for model training. In this scenario, independent validation was also carried out using the data from the 2017–18 season. This was done to check the feasibility of the models in an independent season. Random Forest (RF) and Support Vector Machines (SVM) have various user defined parameters which can be tuned to get the best performance. The RF was tuned for number of trees (*ntree*). Value of *ntree* was varied from 50 to 500 in the interval of 50. Moreover, SVR was tuned for *C* and *Sigma*. The parameter *C* was kept at 0.1, 1, 10, 100, and *Sigma* at 1, 0.1, 0.01, 0.001, and the types of kernel were set as radial basis function. Table 2 shows the performance of models for the first scenario. A comparison between the models shows that RFR performed best in terms of R^2 among all the models, across monthly as well as seasonal level. The comparison of different models of RFR shows that all the models are performing well, with small variation in the R^2 value.

In second scenario the model testing and independent validation was performed on independent season. Table 3 shows the

Model	Data subset	SVR	RFR	MLR
Season	Test	0.68	0.73	0.41
Dec.	Test	0.59	0.61	0.35
Jan.	Test	0.72	0.80	0.48
Feb.	Test	0.72	0.75	0.49
Mar.	Test	0.64	0.76	0.4

Table 2. Performance of the regression models in Scenario 1

Model	Data subset	SVR	RFR	MLR
Season	Test	0.71	0.73	0.44
Season	Validation	0.67	0.67	0.38
Dec.	Test	0.54	0.59	0.34
Dec.	Validation	0.51	0.60	0.31
Jan.	Test	0.69	0.77	0.42
Jan.	Validation	0.54	0.69	0.41
Feb.	Test	0.65	0.75	0.47
Feb.	Validation	0.62	0.69	0.37
Mar.	Test	0.73	0.79	0.49
Mar.	Validation	0.69	0.70	0.45

Table 3. Performance of the regression models in Scenario 2

performance of the various models for the second scenario. We can observe the higher R^2 values on the testing data as compared to the validation data. This was due to the fact that testing data was from the same set of seasons as that of training data, so variations were well captured by the models. The validation data was from the independent season, which caused the slight decline in the R^2. Furthermore, a comparison of monthly and seasonal models revealed that the model created on Jan. data performed best, with an R^2 of 0.80, while R^2 of 0.73, 0.61, 0.75, and 0.76 were attained using RFR for seasonal, Dec., Feb., and Mar. month models, respectively. This demonstrates that both monthly and seasonal models can be used to downscale SM spatially.

3.2 Visual analysis of Original and Downscaled Soil Moisture

A visual comparison between the original 36 km SM and the model downscaled 1 km SM was carried out. The RFR model trained on the seasonal data was applied to the composite stack of India from the 2017-18 season. For comparative analysis, we chose the first composite stack of each month, i.e., Dec., Jan., Feb., and Mar. months. Figure 4 shows the side by side view into original 36 km MS and 1 km downscaled SM. It should be noted that, data was not available for continuous red areas from Jammu and Kashmir state of India. We can observe the granularity and detailed variation of SM in the 1 km downscaled SM data compared to the 36 km SM data. There is a considerable variation in the SM (refer to the blue circle in Figure 4) in the 1 km downscaled SM, whereas such variation was not captured in the 36 km SM data. This shows that 1km downscaled SM can be useful to perform local i.e., sub-district or village level studies, which is not be possible only using the 36 km SM data.

SN	CS End Date	ASM	DSM	Difference
1	3 Jan. 2018	26.3	23.4	-6.1
2	13 Jan. 2018	29.2	30.2	-1
3	3 Feb. 2018	28.8	22.1	6.7
4	23 Feb. 2018	31.1	23.7	7.4
5	6 Mar. 2018	27.5	31.9	-4.4
6	16 Mar. 2018	25.5	34.8	-9.3

ASM-Actual Soil Moisture, DSM-Downscaled Soil Moisture

Table 4. Comparison of actual and downscaled soil moisture

3.3 In-Situ validation using soil moisture sensor Data

We have deployed soil moisture sensors on one of the demo farms located in Pune, maintained by Tata Consultancy Services Limited. The data collected by the sensors (node 3) during the period of December 2017 to March 2018 was used for the validation. Models were trained considering the 3 days composite stacks hence, data available from the sensors was averaged to 3 days to match with frequency and duration of composite stack. Table 4 shows the comparison between actual in-situ SM and downscaled SM estimated by the model for a particular model selection. The comparison table shows that deviations between actual and downscaled soil moisture vary between -9.3 to 7.4 % which is within the acceptable limits. This shows the good agreement between actual and downscaled SM.

4. SUMMARY AND CONCLUSIONS

In this work, we have proposed a machine learning-based soil moisture downscaling approach using the various MODIS products along with the elevation data from SRTM. SM data available at 36 km from SMAP was downscaled to 1 km using the regression-based models. Two scenarios were tested using various regression techniques such as random forest regression, support vector regression, and multivariate linear regression. The results showed that random forest regression-based models performed the best in both scenarios. The performance of various seasonal and monthly models was comparable, with little change in terms of R^2. Visual comparisons of the original 36 km of SMAP soil moisture and the model downscaled 1 km of soil moisture revealed that the downscaled SM provided finer details of SM, which is useful for field or local level studies involving the use of soil moisture, such as drought analysis, hydrological studies and water management decision support. Comparison between downscaled SM and in-situ SM shows the good agreement between the two. The difference in soil moisture between in-situ and downscaled SM was between -9.3 and 7.4 %.

5. FUTURE WORK

As a part of future work, we plan to extend this approach to the *Kharif* season. We have used indices based on optical satellite observations which gets affected by clouds during the *Kharif* season. Attempts are being made to assess the model performance for cloudy conditions of the *Kharif* season.

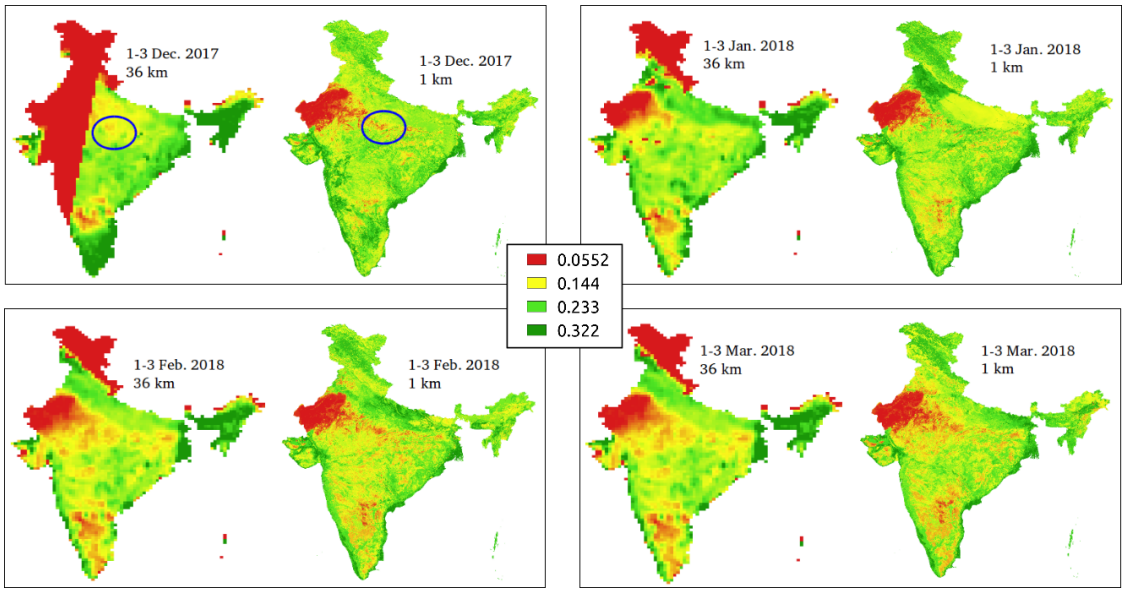

Figure 4. SMAP 36 km vs downscaled 1 km soil moisture maps for India

ACKNOWLEDGEMENTS

We are very thankful to team members of Digital Farming Initiatives (DFI), Tata Consultancy Services Limited. (TCS) for helping us with field observations. Also, we thank our organization, TCS for funding our research.

REFERENCES

Anderson, M. C., Norman, J. M., Mecikalski, J. R., Otkin, J. A., Kustas, W. P., 2007. A climatological study of evapotranspiration and moisture stress across the continental United States based on thermal remote sensing: 1. Model formulation. *Journal of Geophysical Research: Atmospheres*, 112(D10).

Bacchi, O., REICHARDT, K., Oliveira, J., Nielsen, D., 1998. Gamma-ray beam attenuation as an auxiliary technique for the evaluation of the soil water retention curve. *Scientia Agricola*, 55(3), 498–502.

Bastiaanssen, W. G., Molden, D. J., Makin, I. W., 2000. Remote sensing for irrigated agriculture: examples from research and possible applications. *Agricultural water management*, 46(2), 137–155.

Busch, F. A., Niemann, J. D., Coleman, M., 2012. Evaluation of an empirical orthogonal function–based method to downscale soil moisture patterns based on topographical attributes. *Hydrological Processes*, 26(18), 2696–2709.

Chanasyk, D., Naeth, M. A., 1996. Field measurement of soil moisture using neutron probes. *Canadian Journal of Soil Science*, 76(3), 317–323.

Coleman, M. L., Niemann, J. D., 2013. Controls on topographic dependence and temporal instability in catchment-scale soil moisture patterns. *Water Resources Research*, 49(3), 1625–1642.

Das, N. N., Entekhabi, D., Njoku, E. G., 2010. An algorithm for merging SMAP radiometer and radar data for high-resolution soil-moisture retrieval. *IEEE Transactions on Geoscience and Remote Sensing*, 49(5), 1504–1512.

Dean, T., Bell, J., Baty, A., 1987. Soil moisture measurement by an improved capacitance technique, Part I. Sensor design and performance. *Journal of Hydrology*, 93(1-2), 67–78.

Gorelick, N., Hancher, M., Dixon, M., Ilyushchenko, S., Thau, D., Moore, R., 2017. Google Earth Engine: Planetary-scale geospatial analysis for everyone. *Remote Sensing of Environment*. https://doi.org/10.1016/j.rse.2017.06.031.

Ines, A. V., Droogers, P., 2002. Inverse modelling in estimating soil hydraulic functions: a Genetic Algorithm approach. *Hydrology and Earth System Sciences*, 6(1), 49–66.

Jacquette, E., Al Bitar, A., Mialon, A., Kerr, Y., Quesney, A., Cabot, F., Richaume, P., 2010. Smos catds level 3 global products over land. *Remote Sensing for Agriculture, Ecosystems, and Hydrology XII*, 7824, International Society for Optics and Photonics, 78240K.

Jarvis, A., Reuter, H. I., Nelson, A., Guevara, E. et al., 2008. Hole-filled SRTM for the globe Version 4, available from the CGIAR-CSI SRTM 90m Database.

Joseph, M., Oakley, M., Schira, Z., 2019. smapr: Acquisition and Processing of NASA Soil Moisture Active-Passive (SMAP) Data. R package version 0.2.1.

Kaheil, Y. H., Gill, M. K., McKee, M., Bastidas, L. A., Rosero, E., 2008. Downscaling and assimilation of surface soil moisture using ground truth measurements. *IEEE Transactions on Geoscience and Remote Sensing*, 46(5), 1375–1384.

Kerr, Y. H., Waldteufel, P., Wigneron, J.-P., Martinuzzi, J., Font, J., Berger, M., 2001. Soil moisture retrieval from space: The Soil Moisture and Ocean Salinity (SMOS) mission. *IEEE transactions on Geoscience and remote sensing*, 39(8), 1729–1735.

Ledieu, J., De Ridder, P., De Clerck, P., Dautrebande, S., 1986. A method of measuring soil moisture by time-domain reflectometry. *Journal of Hydrology*, 88(3-4), 319–328.

Liu, Y. Y., Parinussa, R., Dorigo, W. A., De Jeu, R. A., Wagner, W., Van Dijk, A., McCabe, M. F., Evans, J., 2011. Developing

an improved soil moisture dataset by blending passive and active microwave satellite-based retrievals. *Hydrology and Earth System Sciences*, 15(2), 425–436.

Liu, Y., Yang, Y., Jing, W., Yue, X., 2017. Comparison of different machine learning approaches for monthly satellite-based soil moisture downscaling over Northeast China. *Remote Sensing*, 10(1), 31.

Malbéteau, Y., Merlin, O., Molero, B., Rüdiger, C., Bacon, S., 2016. DisPATCh as a tool to evaluate coarse-scale remotely sensed soil moisture using localized in situ measurements: Application to SMOS and AMSR-E data in Southeastern Australia. *International Journal of Applied Earth Observation and Geoinformation*, 45, 221–234.

Naeimi, V., Scipal, K., Bartalis, Z., Hasenauer, S., Wagner, W., 2009. An improved soil moisture retrieval algorithm for ERS and METOP scatterometer observations. *IEEE Transactions on Geoscience and Remote Sensing*, 47(7), 1999–2013.

NPI, N., 2022. Agriculture. https://www.india.gov.in/topics/agriculture.

Ochsner, E., Cosh, M. H., Cuenca, R., Hagimoto, Y., Kerr, Y. H., Njoku, E., Zreda, M. et al., 2013. State of the art in large-scale soil moisture monitoring. *Soil Science Society of America Journal*, 1–32.

Owe, M., de Jeu, R., Holmes, T., 2008. Multisensor historical climatology of satellite-derived global land surface moisture. *Journal of Geophysical Research: Earth Surface*, 113(F1).

O'Neill, P. E., Chan, S., Njoku, E. G., Jackson, T., Bindlish, R., Chaubell, J., 2019. Smap l3 radiometer global daily 36 km ease-grid soil moisture. *Version*, 6.

Pandit, A., Sawant, S., Mohite, J., Pappula, S., 2020. A data-driven approach for bare surface soil moisture estimation using Sentinel-1 SAR data and ground observations. *Geocarto International*, 1–30.

Peng, J., Loew, A., Merlin, O., Verhoest, N. E., 2017. A review of spatial downscaling of satellite remotely sensed soil moisture. *Reviews of Geophysics*, 55(2), 341–366.

Robinson, D., Campbell, C., Hopmans, J., Hornbuckle, B. K., Jones, S. B., Knight, R., Ogden, F., Selker, J., Wendroth, O., 2008. Soil moisture measurement for ecological and hydrological watershed-scale observatories: A review. *Vadose Zone Journal*, 7(1), 358–389.

Robock, A., Vinnikov, K. Y., Srinivasan, G., Entin, J. K., Hollinger, S. E., Speranskaya, N. A., Liu, S., Namkhai, A., 2000. The global soil moisture data bank. *Bulletin of the American Meteorological Society*, 81(6), 1281–1300.

Schaaf, C., Wang, Z., 2015. MCD43A3/MODIS. *Terra+ Aqua BRDF/Albedo Daily L3 Global–500m V006 500m Grid, Version*, 6.

Seneviratne, S. I., Corti, T., Davin, E. L., Hirschi, M., Jaeger, E. B., Lehner, I., Orlowsky, B., Teuling, A. J., 2010. Investigating soil moisture–climate interactions in a changing climate: A review. *Earth-Science Reviews*, 99(3-4), 125–161.

Sheng, J., Rao, P., Ma, H., 2019. Spatial downscaling of the fy3b soil moisture using random forest regression. *2019 8th International Conference on Agro-Geoinformatics (Agro-Geoinformatics)*, IEEE, 1–6.

Vermote, E., Wolfe, R., 2015. Mod09ga modis/terra surface reflectance daily l2g global 1km and 500m sin grid v006 [data set]. nasa eosdis land processes daac.

Vinnikov, K. Y., Yeserkepova, I., 1991. Soil moisture: Empirical data and model results. *Journal of Climate*, 66–79.

Wagner, W., Blöschl, G., Pampaloni, P., Calvet, J.-C., Bizzarri, B., Wigneron, J.-P., Kerr, Y., 2007. Operational readiness of microwave remote sensing of soil moisture for hydrologic applications. *Hydrology Research*, 38(1), 1–20.

Wagner, W., Dorigo, W., de Jeu, R., Fernandez, D., Benveniste, J., Haas, E., Ertl, M. et al., 2012. Fusion of active and passive microwave observations to create an essential climate variable data record on soil moisture. *ISPRS Annals of the Photogrammetry, Remote Sensing and Spatial Information Sciences (ISPRS Annals)*, 7, 315–321.

Wan, Z., 2015. University of California Santa Barbara, Simon Hook, Glynn Hulley-JPL and MODAPS SIPS-NASA. *MOD11A1 MODIS/Terra Land Surface Temperature and the Emissivity Daily L3 Global 1km SIN Grid. NASA LP DAAC*.

Zhang, D., Zhou, G., 2016. Estimation of soil moisture from optical and thermal remote sensing: A review. *Sensors*, 16(8), 1308.